In vitro degradation of a chitosan-based osteochondral construct points to a transient effect on cellular viability

To cite this article: Katherine Pitrolino *et al* 2024 *Biomed. Mater.* **19** 055025

Biomedical Materials

PAPER

In vitro degradation of a chitosan-based osteochondral construct points to a transient effect on cellular viability

Katherine Pitrolino[1,2], **Reda Felfel**[3,4,5], **George Roberts**[3], **Colin Scotchford**[3], **David Grant**[3,*] and **Virginie Sottile**[6,7,*]

[1] School of Medicine, University of Nottingham, Nottingham, United Kingdom
[2] College of Science and Engineering, University of Derby, Derby, United Kingdom
[3] Advanced Materials Research Group, Faculty of Engineering, University of Nottingham, Nottingham, United Kingdom
[4] Mechanical and Aerospace Engineering, University of Strathclyde, Glasgow, United Kingdom
[5] Physics Department, Faculty of Science, Mansoura University, Mansoura, Egypt
[6] Department of Molecular Medicine, University of Pavia, Pavia, Italy
[7] UOC Bioscaffolds and transplantation, Fondazione IRCCS Policlinico San Matteo, Pavia, Italy
* Authors to whom any correspondence should be addressed.

E-mail: david.grant@nottingham.ac.uk and virginie.sottile@unipv.it

OPEN ACCESS

RECEIVED
21 February 2024

REVISED
18 June 2024

ACCEPTED FOR PUBLICATION
18 July 2024

PUBLISHED
6 August 2024

Keywords: chitosan, scaffold, degradation, glucosamine, osteochondral repair

Supplementary material for this article is available online

Abstract

Bioresorbable chitosan scaffolds have shown potential for osteochondral repair applications. The *in vivo* degradation of chitosan, mediated by lysozyme and releasing glucosamine, enables progressive replacement by ingrowing tissue. Here the degradation process of a chitosan-nHA based bioresorbable scaffold was investigated for mass loss, mechanical properties and degradation products released from the scaffold when subjected to clinically relevant enzyme concentrations. The scaffold showed accelerated mass loss during the early stages of degradation but without substantial reduction in mechanical strength or structure deterioration. Although not cytotoxic, the medium in which the scaffold was degraded for over 2 weeks showed a transient decrease in mesenchymal stem cell viability, and the main degradation product (glucosamine) demonstrated a possible adverse effect on viability when added at its peak concentration. This study has implications for the design and biomedical application of chitosan scaffolds, underlining the importance of modelling degradation products to determine suitability for clinical translation.

1. Introduction

Tissue engineering and regenerative medicine promise a step change in treatment options for defects such as non-union bone fractures and osteochondral lesions (Bedi *et al* 2010, Levengood and Zhang 2014, Tribe *et al* 2017, Marshall *et al* 2023, Angolkar *et al* 2024). Several osteochondral tissue engineered devices have been used in clinical trials (BSTCargel (Stanish *et al* 2013), Neocart (GlobeNewswire 2018), Salucartilage (Lange *et al* 2006), MaioRegen (Christensen *et al* 2016), Trufit (Verhaegen *et al* 2014)) and while these products showed encouraging signs at early timepoints, they largely failed to achieve reliable tissue repair and full functionality in the long term (GlobeNewswire 2018, Lange *et al* 2006, Christensen *et al* 2016, Verhaegen *et al* 2014, Hulsart-Billstrom *et al* 2016). The ability of osteochondral scaffolds to integrate with the surrounding tissue and progressively degrade while being replaced by regenerated tissue is key to cartilage and bone repair applications (Koons *et al* 2020, Collins *et al* 2021).

Typical bone and cartilage products have centred on collagen-based devices, including CaRes (Schneider *et al* 2011), MACI (Nawaz *et al* 2014), MaioRegen (Kon *et al* 2010), Chondro-Gide (McCarthy and Roberts 2013), Osseofit (McCarrel *et al* 2017) and Vericart (GlobeNewswire 2018). Although able to initiate articular cartilage repair and showing promise in applications such as Autologous Chondrocyte Implantation (ACI) (Schneider *et al* 2011, McCarthy and Roberts 2013), many of these products failed to sustain osteochondral tissue

regeneration (Christensen *et al* 2016, GlobeNewswire 2018), leading to further surgical interventions after 2–5 years follow up (Wylie *et al* 2016). Collagen is known to degrade quickly, for example, CaRes shows full mass loss in 24 weeks (Schneider *et al* 2011), although there is limited information on the kinetics and precise products released during the degradation process (Schneider *et al* 2011).

An alternative natural biomaterial with slower degradation rates than collagen and structural similarities with glycoaminoglycans present in cartilage, is chitosan (Martinez *et al* 2015, Fourie *et al* 2022, Piaia *et al* 2024). It is a derivative of chitin, the long chain polysaccharide of the monomer N-acetyl-D-glucosamine (Croisier and Jérôme 2013). Chitin is abundant in nature and can be extracted from fungi or from the outer skeletons of crustaceans. Deacetylation of the chitin polymer to chitosan (Notara *et al* 2009, Croisier and Jérôme 2013) allows the formation of gels and membranes, with varying degrees of deacetylation conferring distinct material properties for use in tissue engineered applications (Di Martino *et al* 2005, Croisier and Jérôme 2013, Levengood and Zhang 2014, Pitrolino *et al* 2022).

The present study analyses the degradation of a porous bi-layered chitosan scaffold (Pitrolino *et al* 2022), which recapitulates the architecture of native articular cartilage and subchondral bone. The bone-like layer was supplemented with 70 wt% nano-hydroxyapatite (nHA) rods to improve osteoinduction and enhance mechanical strength (Thein-Han and Misra 2009). To investigate how scaffold degradation may impact on the potential use for osteochondral applications, the degradation of a porous chitosan scaffold was monitored *in vitro* under different experimental conditions. Chitosan is known to degrade mainly by enzymatic hydrolysis, therefore the effect of enzymes present in vivo, i.e. lysozyme and N-acetylglucosaminindase (NAG), were considered. These enzymes were used separately and in combination at concentrations detected in the human body, i.e. Lysozyme (120 mg l^{-1}, (Bennett and Skosey 1977)) and N-Acetylglucosaminidase (6.8 U l^{-1}, (Lim *et al* 2008)). The degradation products released at pre-determined time-points were quantified and tested on human mesenchymal stem cells (MSC) *in vitro* to analyse their effect.

2. Method

2.1. Materials

The stock aqueous solutions were prepared from chitosan powder (CS) from Weifeng Kehai, China (MW 471 kDa, degree of deacetylation (DD) 84% ± 2%), glacial acetic acid from Sigma-Aldrich, Dorset, UK and Genipin (GN) from Guangxi Shanyun Biochemical Science and Technology Co., China. Polycaprolactone (PCL) (MW: 14 kDa), dichloromethane, polyvinyl alcohol (PVA, MW: 13–23 kDa, 87%–89% hydrolysed), potassium hydroxide pellets, sodium borohydride solution (99%), lysozyme from chicken egg white (⩾ 95 %) and NAG (⩾ 10 units/mg protein) were obtained from Sigma. Nano-hydroxyapatite rods from a 14.5% (w/v) suspension (nHA, Promethean Particles, Nottingham, UK) were used as described previously (Pitrolino *et al* 2022). Reagents used for cell culture as stated below were purchased from Thermo Fisher Scientific (Loughborough, UK).

Table 1. Enzyme Concentrations for Degradation studies.

Solution	Enzyme	Concentration
PBS	None	N/A
PBS + L	Lysozyme	120 mg l^{-1}
PBS + NAG	N-Acetylglucosaminindase	6.8 U l^{-1}
PBS + LNAG	Lysozyme and N-Acetylglucosaminindase	120 mg l^{-1} 6.8 U l^{-1}

2.2. Scaffold production

Chitosan-genipin (Chitosan) and chitosan-genipin-nano-Hydroxyapatite (Chitosan-nHA) scaffolds, containing 2.5% GN wrt chitosan, were manufactured as detailed previously (Pitrolino *et al* 2022), to produce a bilayer porous device with ∼92% porosity. Each layer contained a 4% acetic solution of chitosan, GN and PCL microspheres as porogen. The manufacturing method, utilising cross-linking, freeze-drying and particle leaching-out techniques, created a scaffold with differential pore size using PCL microspheres (180–300 μm and 300–425 μm). To produce the chitosan-nHA composite scaffold, a suspension of nHA rods was incorporated at 70% (w/w wrt CS) in the CS solution and PCL (300–425 μm) porogen mixture before cross-linking.

2.3. Mass loss

The degradation kinetics of the chitosan scaffold was measured at regular intervals (day 0, 3, 7, 14, 21, 28) according to BS ISO 13781. Briefly, five dry scaffolds, approximately 0.04 g in weight, 14 mm in height and 7 mm in diameter, were submersed in individually capped glass vials containing 20 ml of either (i) PBS; (ii) PBS with chicken egg white lysozyme (PBS + L) (120 mg l^{-1})); (iii) PBS with N-acetyl-β-glucosaminidase (6.8 U/l) (PBS + NAG); or (iv) PBS with both lysozyme and NAG, (PBS + LNAG) as shown in table 1.

Vials were stored at 37 °C, and the scaffolds were tested at regular intervals for weight loss. The degradation solution was replaced after each test. The scaffolds were dried in a vacuum oven at 50 °C for at least 2 h to determine the initial dry weight (W_o), the final dry weight (W_t) was measured at each timepoint. The chitosan-nHA scaffold was tested at the same frequency as the chitosan scaffold, the initial mass of the chitosan-nHA was adjusted for the increased starting

weight of the added nHA. The percentage remaining mass was calculated using the following equation:

$$\frac{(W_o - W_t)}{W_o} \times 100.$$

2.4. Mechanical properties

An INSTRON 5966 (Instron Universal Testing Instruments, Buckinghamshire, UK) compression-testing machine fitted with a 100 N load cell and set at 0.5 mm/min crosshead speed was used to test the mechanical properties of both types of chitosan scaffold under ambient conditions. Strain was calculated from the compressive extension and compressive stress was calculated from the load data recorded from the equipment software using the accurate scaffold dimensions. Stress-strain curves were generated, and compressive modulus was calculated using the gradient of the stress/strain data within the initial linear region. Compressive strength was determined as the maximum compressive stress at 20% strain. Five hydrated samples (approximately 14 mm in length and 7 mm in diameter) were tested applying 20% strain in each case (Felfel *et al* 2018, Pitrolino *et al* 2022). Parameters analysed are summarised in supplementary table 2.

2.5. Imaging

The morphology of the chitosan and chitosan-nHA scaffolds (2 mm slices) was examined after exposure to degradation fluid using variable pressure mode SEM at each degradation timepoint up to 14 d, using a Quanta FEG 650 scanning electron microscope operating at 10 kV, 770 Pa. The pore size of the scaffold was determined from PenTabletDrive software (Huion, Shenzhen, China) by measuring the diameter of all pores ($n = 9$) in eSEM images at 0, 3 and 7 d (Sarem *et al* 2013, Siddiqui *et al* 2015).

2.6. Analysis of degradation products—HPLC

The supernatant from the mass loss study of the chitosan-nHA scaffold was collected and analysed at each timepoint (day 0, 3, 7, 14, 21) for pH and chemical composition. The pH measurements were carried out using a FiveEasy FE20 pH meter (Mettler-Toledo, Leicester, UK).

To determine the chemical composition, the degradation products were analysed by high performance liquid chromatography using an Agilent 1200 infinity (HPLC, Agilent Technologies, Cheshire, UK) fitted with an Aminex column HPX-87 C (Bio-Rad, Hertfordshire, UK) using an isocratic 0.005 M sulphuric acid mobile phase. The pump ran at 0.4 ml/min with an injection volume between 20 and 40 µl. Standards were made using solutions of CS, GN, glucosamine hydrochloride (Sigma-Aldrich), NAG and glucose (BDH, Poole, UK) at the concentrations shown in supplementary table 1; methanol, ethanol, PBS and purified water were also used as standards. Elution peaks were detected by refractive index and the spectra were recorded for 40 min.

2.7. Cell culture

Immortalised human bone marrow-derived MSCs labelled with GFP (as described in Harrison *et al* 2017, Pitrolino *et al* 2022) were cultured in standard growth medium (SM) consisting of Dulbecco's Modified Eagle's Medium supplemented with 10% (v/v) foetal bovine serum, 1% (v/v) non-essential amino acids, 1% (v/v) L-Glutamine, and 0.5% (v/v) penicillin/streptomycin, with medium changed every 2–3 d. The cells were passaged using 0.25% trypsin/0.02% EDTA and maintained at 37 °C in 5% CO_2.

2.8. Glucosamine dose-response tests

Media supplemented with different concentrations of glucosamine (0, 2, 20 and 200 mM) were added to MSCs cultured in 96-well plates over 48 h, before performing DNA content and metabolic activity measurements as detailed below.

2.9. Cell metabolic activity

The metabolic activity was assayed using a PrestoBlue Cell Viability Reagent (Thermo Fisher Scientific) according to the manufacturer's instruction as previously described (Macri-Pellizzeri *et al* 2018). Fluorescence intensity was measured using a TECAN Infinite M200 plate reader (Tecan, Switzerland) at 560 nm excitation/590 nm emission with a constant gain of 85%.

2.10. Cell DNA content

DNA content was analysed using the Quant-IT PicoGreen assay kit (Thermo Fisher Scientific) as previously described (Macri-Pellizzeri *et al* 2018), fluorescence was measured using a TECAN Infinite M200 plate reader (480 nm excitation/520 nm emission) and quantified using a DNA standard curve.

2.11. Degradation supernatant—cytotoxicity

Cytotoxicity measurements were performed according to ISO 10 993–5 and 10 993–12. Scaffolds were degraded on a plate shaker using the conditions described in Mass Loss, however, PBS was replaced with SM to enable cell culture experiments. Each scaffold was incubated in 4 ml of SM based on the ISO recommended volumes for a porous device. The degradation supernatant was collected at days 1, 2, 4, 7, 14, 21, 28 and stored at −20 °C until use. SM with 5% Dimethylsuphoxide (Sigma-Aldrich) was used as positive cytotoxic control, fresh SM was used as a negative cytotoxic control, and SM incubated without the scaffold was used as a blank. MSCs were seeded in triplicate for each condition onto 96-well

plates at a concentration of 30 000 cells/well and incubated for 24 h. The scaffold-conditioned medium (100 µl/well) was added for 48 h before imaging and cell viability evaluation through metabolic activity and DNA content measurements, with a reduction in cell viability of 30% considered as a cytotoxic effect.

2.12. Statistical analysis

The results are represented as mean ± SEM (standard error of the mean) from at least 5 replicates ($n \geqslant 5$), unless otherwise stated. All graphs and statistical analyses were performed using GraphPad Prism 6.0. The data was analysed using two-way ANOVA with Tukey post hoc testing for multiple comparisons and the statistical difference between conditions is shown, with p values as $^{*}\leqslant 0.05$, $^{**}\leqslant 0.01$, $^{***}\leqslant 0.001$, $^{****}\leqslant 0.0001$.

3. Results

3.1. Mass loss

Chitosan hydrogels and scaffolds degrade by hydrolytic mechanisms (Roberts 1992) that are accelerated by enzymes (Vårum *et al* 1997). To determine the specific degradation kinetics of the chitosan and chitosan-nHA scaffolds, mass loss was measured over 28 d using four different conditions: PBS, PBS + L, PBS + NAG and PBS + LNAG. The largest single change in mass loss occurred between day 0 and day 3 for both scaffolds, accounting for between 84%–94% and 36%–44% of the total mass loss at day 28 for the chitosan and chitosan-nHA scaffolds respectively (figure 1). Using the adjusted mass loss figure to account for the increased starting weight of the chitosan-nHA scaffold, the mass loss at day 3 was between 9%–11% for the chitosan scaffold and between 3%–6% for the chitosan-nHA scaffold. After day 3, the cumulative mass loss for both scaffolds increased, reaching between 10%–14% total mass loss for the chitosan scaffold and between 12%–16% for the chitosan-nHA scaffold at day 28. There was a significant variation between the degradation conditions tested for both scaffolds. The addition of lysozyme to PBS increased the mass loss significantly compared to PBS alone, reaching a 38% (figure 1(A)) and a 33% (figure 1(B)) increase at day 28 for the chitosan and chitosan-nHA scaffold respectively. The addition of NAG to PBS did not have a significant effect, and the presence of both enzymes mirrored the increase observed using lysozyme, with no significant difference between PBS + L and PBS + LNAG for both scaffolds (figures 1(A) and (B).

3.2. Mechanical properties

To determine how the observed mass loss affected the strength of the scaffold, the mechanical properties of both the chitosan and chitosan-nHA scaffold were measured throughout the degradation process and compared with the initial values measured before immersion in the degradation solutions. Compressive strength (figure 2(A)) increased from 4 kPa at day 0 to between 6–7 kPa at day 3 returning similar values up to 21 d. The compressive modulus (figure 2(B)) increased from between 13–14 kPa at day 0 to between 15–24 kPa at day 3. There was no significant difference in scaffold compressive strength or modulus when these were placed in the different degradation solutions.

3.3. Imaging

To determine the effect of degradation on construct morphology, the chitosan-only and chitosan-nHA layers were imaged separately using variable pressure mode SEM (figure 3). The images showed deterioration in pore structure and a slight pore widening over time in both chitosan-only and chitosan-HA scaffolds, measured to increase marginally from an average of 184 ± 22 µm at day 0–229 ± 21 µm at day 3 for the chitosan-only layer, and from 264 ± 54 µm at day 0–313 ± 56 µm at day 3 for the chitosan-nHA layer.

3.4. Analysis of degradation products

To identify and quantify the scaffold degradation products, the degradation supernatant from the chitosan-nHA scaffold was collected and analysed by HPLC at each timepoint (figure 4). Glucose was only detected between day 1 and day 3 and at low concentrations of < 0.5 mM. There was a spike of glucosamine (170 mM) measured at day 7, followed by lower concentrations of glucosamine (2 mM) and N-acetylglucosamine (3 mM) detected at day 14 and day 21. The pH of the supernatant was around 7.4 at early timepoints (day 2, 3 and 7) and then decreased to around 6.4 at day 14, before stabilising by day 21 to a mean of 6.5.

3.5. Analysis of cellular response to glucosamine

Based on the profile of glucosamine release, the effect of increasing concentrations of this compound was analysed on human MSCs, the progenitor cell type present at the intended implantation site, to determine the suitability of the device for the repair of osteochondral defects. Cells were exposed to concentrations of glucosamine between 0–200 mM to determine the effect on cell viability. All glucosamine concentrations significantly inhibited cell viability over 48 h when compared to untreated MSCs cultures, in a concentration dependent manner (figure 5).

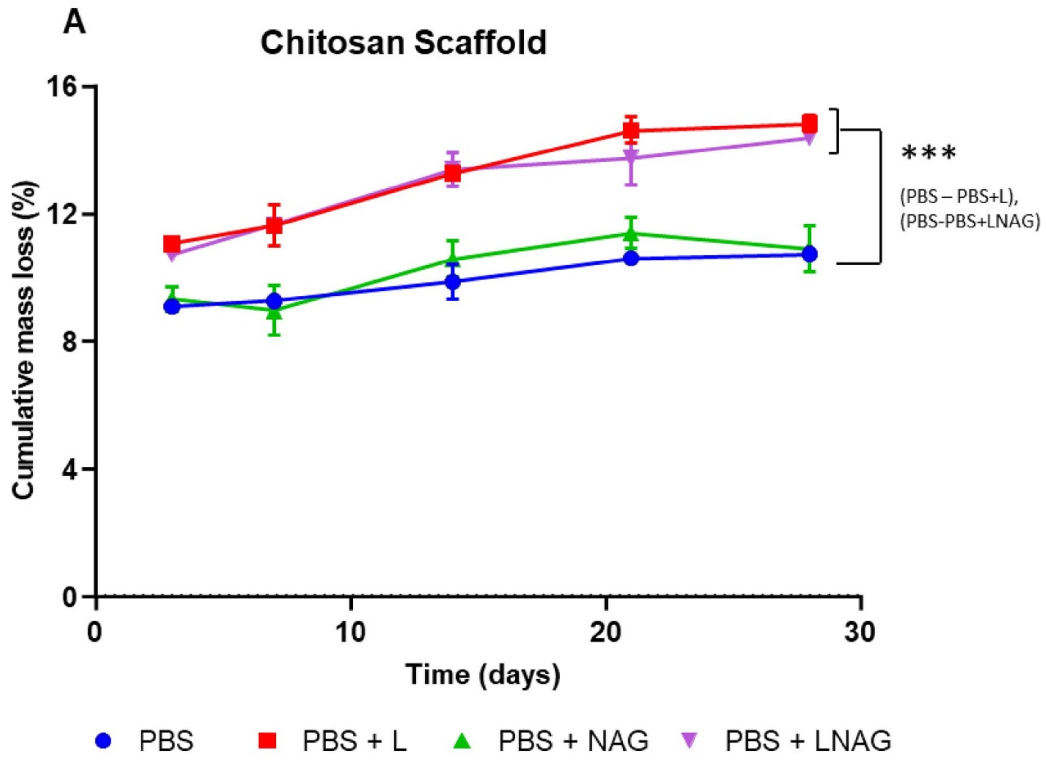

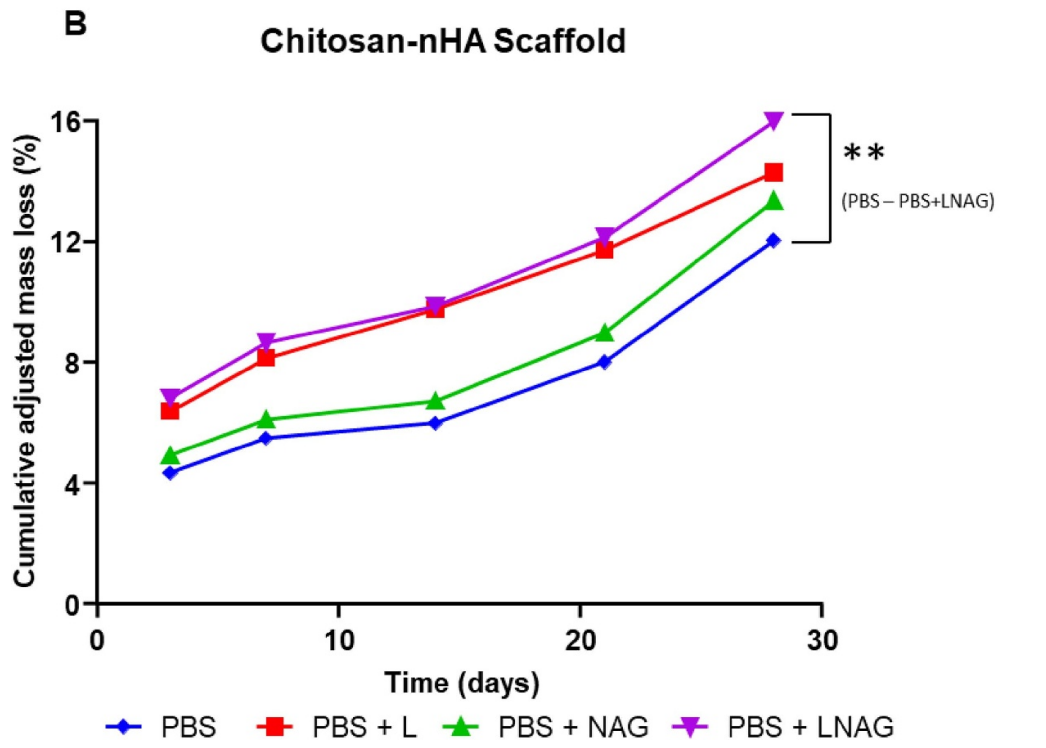

Figure 1. Mass loss of chitosan (A) and chitosan-nHA (B) composite scaffolds after degradation at 37 °C with PBS and lysozyme (120 mg l^{-1}) and N-Acetylglucosaminidase (6.8 μg/L). Graphs A & B show the mass loss at time-points 0, 3, 7, 14, 21, 28 d. Results are expressed as mean ± standard error of the mean, $n = 3$. A significant difference is shown between conditions, PBS and PBS + L, and PBS and PBS + LNAG, for the chitosan scaffold (A) and between conditions PBS and PBS + LNAG, for the chitosan-nHA scaffold (B), $^{**}p \leqslant 0.01$, $^{***}p \leqslant 0.001$.

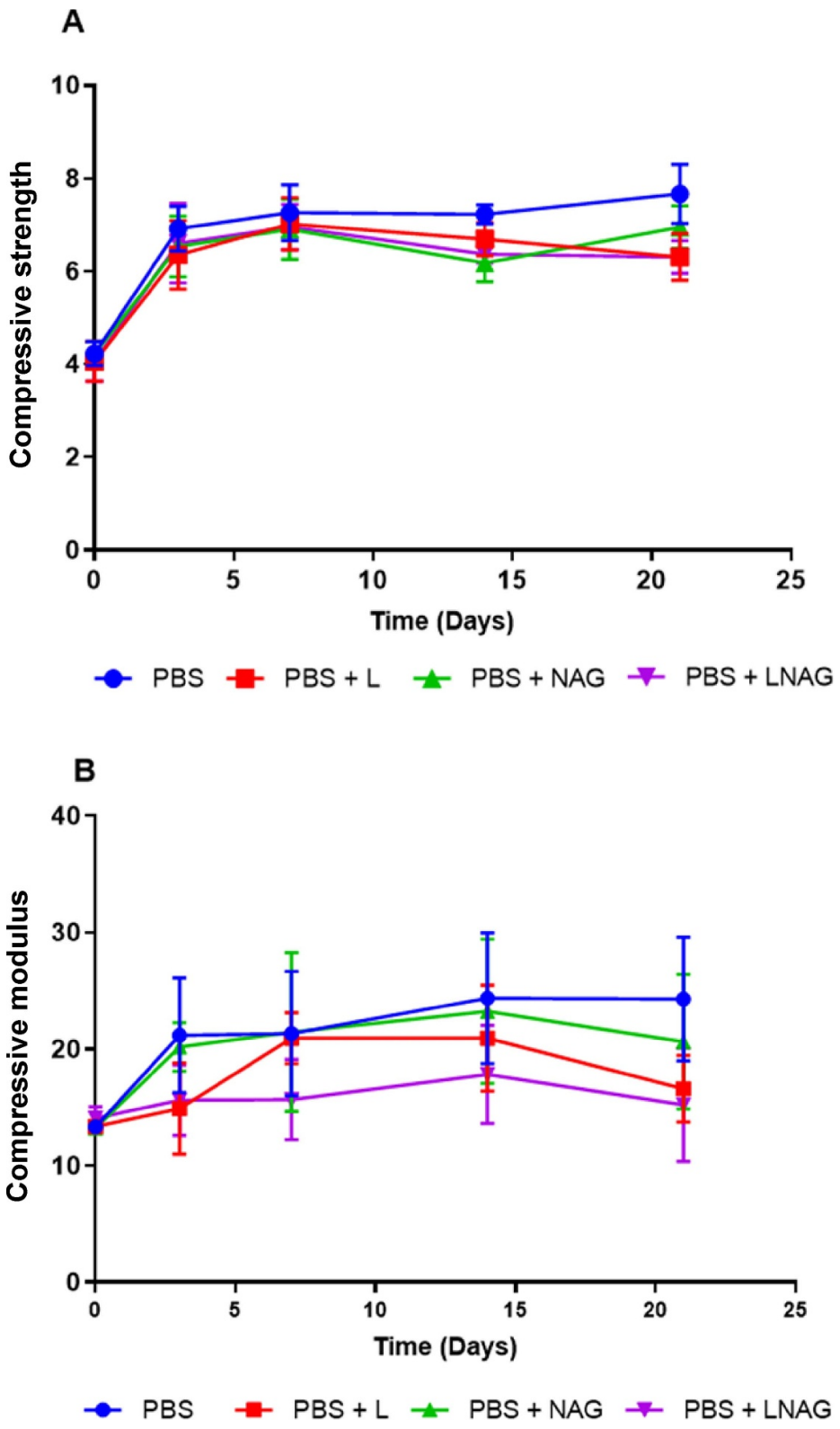

Figure 2. Mechanical strength (A) and compressive modulus (B) of chitosan-nHA scaffolds analysed over 21 d after immersion in PBS solution or PBS solution with enzymes. Results are expressed as mean ± standard error of the mean, $n = 3$, no significant difference found between conditions.

DNA measurements indicated a 3-fold decrease in cell number when culture medium was supplemented with 2 mM glucosamine compared to the control, and a 40-fold decrease when supplemented with 200 mM glucosamine (figure 5(A)). Likewise, the metabolic activity at 48 h also showed a dose-dependent reduction with increasing concentrations of glucosamine (figure 5(B)).

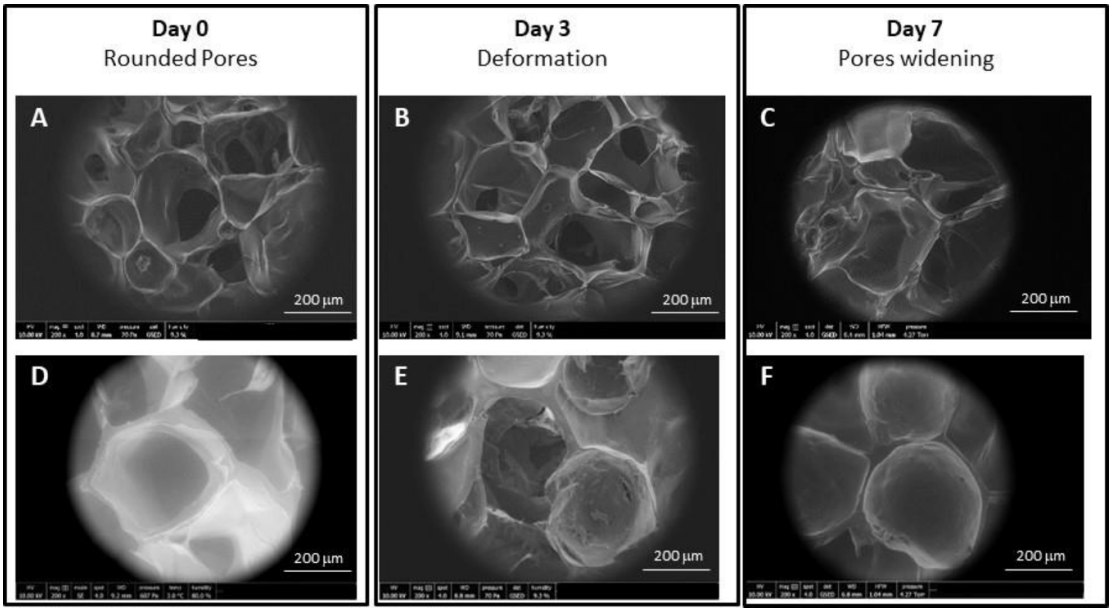

Figure 3. Scaffold internal pore structure imaged by eSEM after degradation in PBS at day 0, 3 and day 7, showing chitosan (A-C) and chitosan-nHA (D-F) layers. Scale bar shows 200 µm.

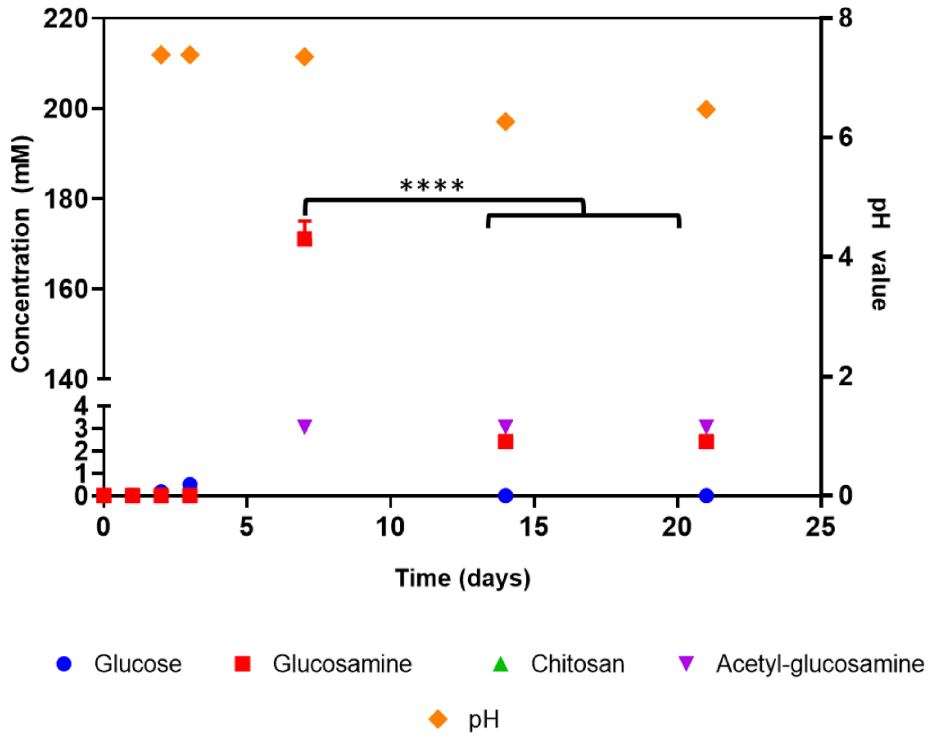

Figure 4. HPLC analysis of the concentration of degradation products and pH of degradation supernatant measured over 21 d after chitosan-nHA scaffolds were immersed in aqueous solution. Results are expressed as the mean ± standard error of the mean, $n = 3$, comparison between concentration of degradation products, **** $p \leqslant 0.0001$.

3.6. Cytotoxicity analysis of cellular response to degradation supernatant

The effect of the degradation supernatant was also analysed on MSCs using the chitosan-nHA scaffold according to ISO 10 993–12 (figure 6). Conditioned medium collected over a 4-week period (1, 2, 4, 7, 14, 21 and 28 d) was used in order to monitor the effects of degradation products emerging in the early, mid and later phases of the process. There was a decrease in DNA content (figure 6(A)) when the cells were exposed to scaffold-conditioned media from day 14 and day 21 of the degradation trials. The DNA content recorded for cultures exposed to day 1 scaffold-conditioned medium was also significantly lower than for all later timepoints, falling below the cytotoxicity threshold.

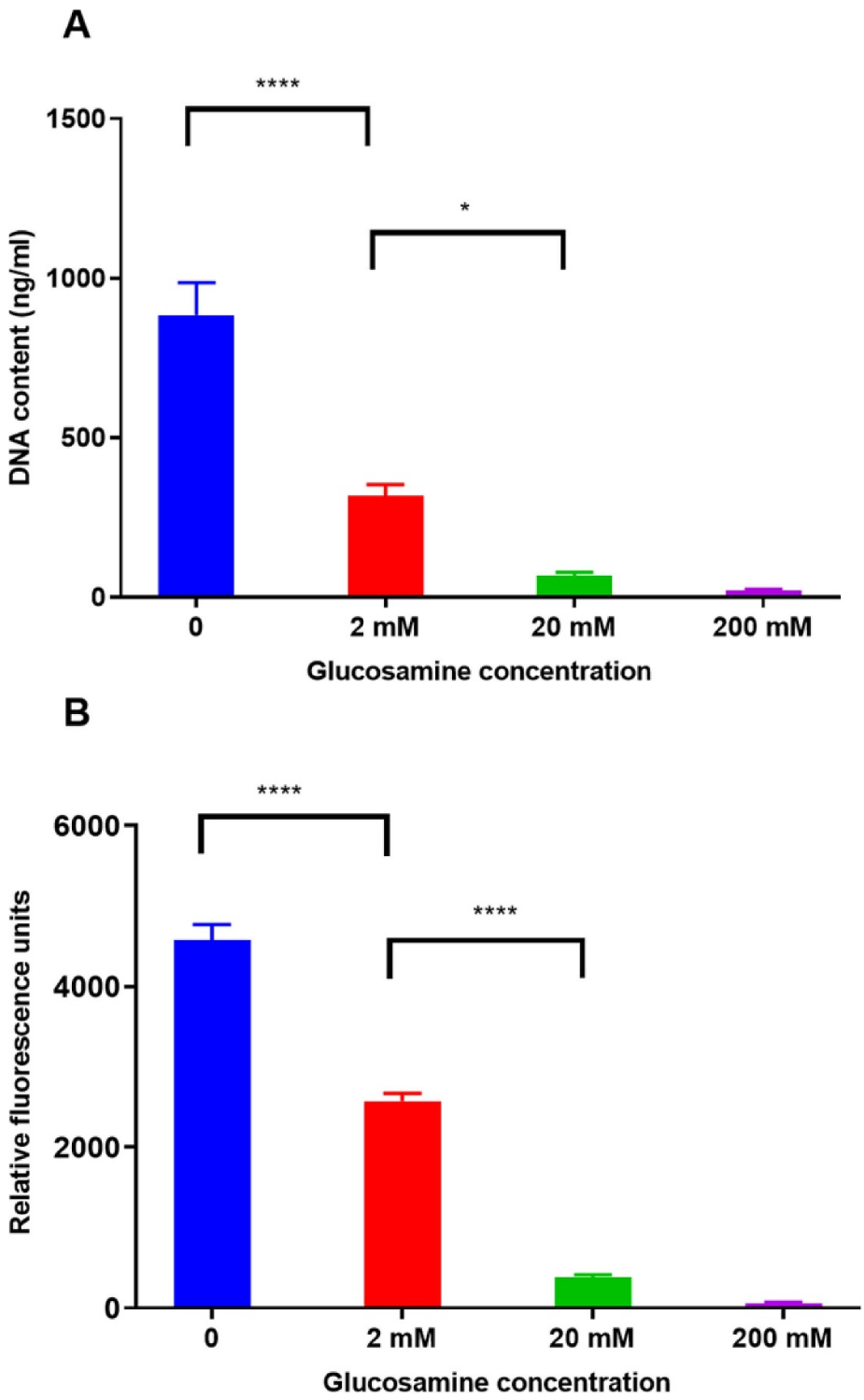

Figure 5. Effect of glucosamine supplementation on MSC cultures over 48 h period analysed by measuring DNA content (A) and cell metabolic activity (B). Results are expressed as the mean ± standard error of the mean, $n = 3$, * $p \leqslant 0.05$, **** $p \leqslant 0.0001$.

Cell metabolic activity measurements (figure 6(B)) showed a slight non-significant decrease for cells exposed to scaffold-conditioned medium compared to the control, for all degradation timepoints up to day 7, although this was within the ISO cytotoxic threshold (70% of the control value). When day 14 scaffold-conditioned medium was used, the metabolic activity of the cells showed a significant decrease and came close to the cytotoxic threshold. Microscopy observation supported these findings (figure 7), as cultures exposed to day 14 degradation medium displayed lower cell numbers than the matching negative control, while there was no visible difference in cell density for cells exposed to medium from day 4.

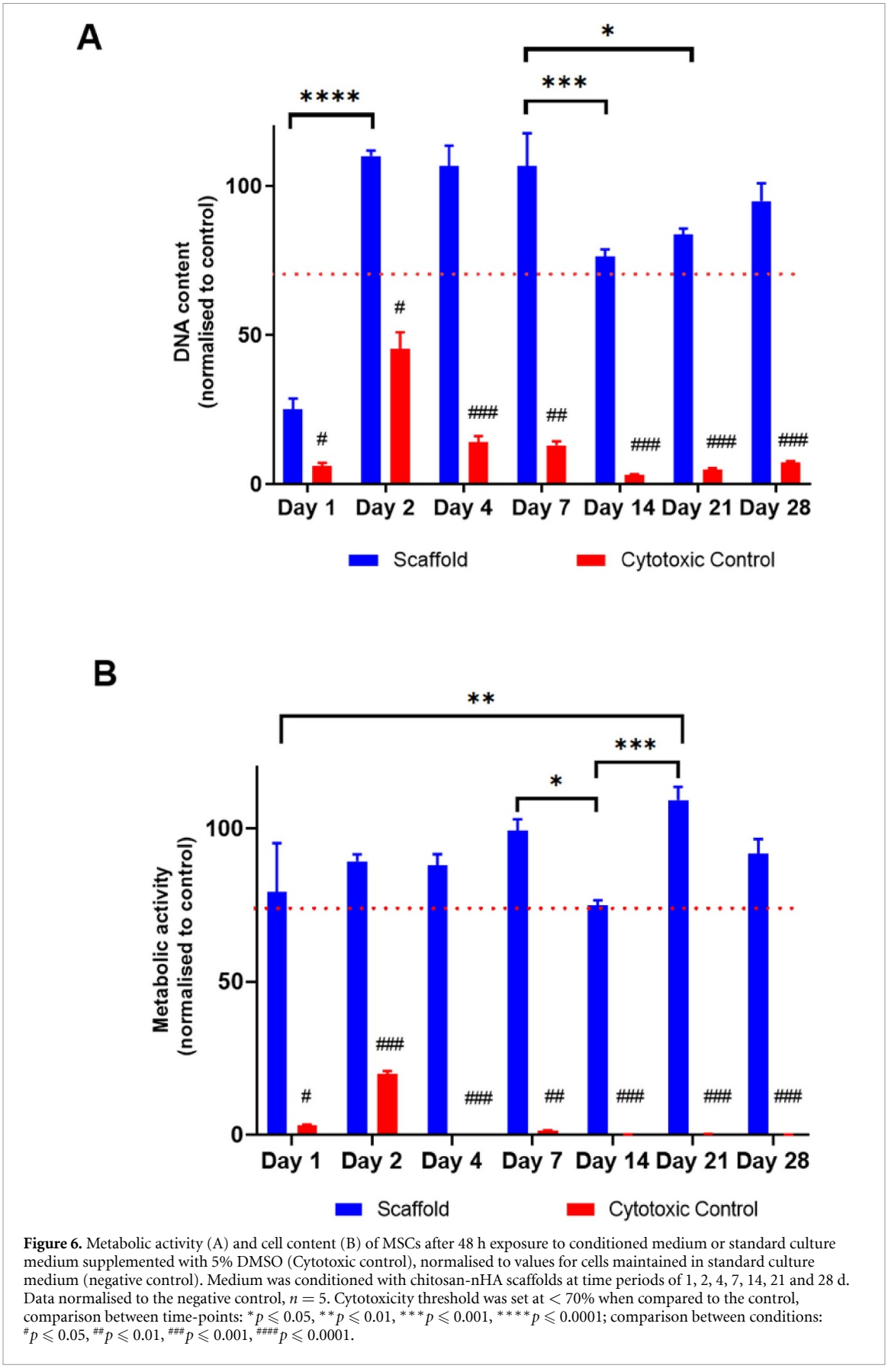

Figure 6. Metabolic activity (A) and cell content (B) of MSCs after 48 h exposure to conditioned medium or standard culture medium supplemented with 5% DMSO (Cytotoxic control), normalised to values for cells maintained in standard culture medium (negative control). Medium was conditioned with chitosan-nHA scaffolds at time periods of 1, 2, 4, 7, 14, 21 and 28 d. Data normalised to the negative control, $n = 5$. Cytotoxicity threshold was set at $< 70\%$ when compared to the control, comparison between time-points: $^{*}p \leqslant 0.05$, $^{**}p \leqslant 0.01$, $^{***}p \leqslant 0.001$, $^{****}p \leqslant 0.0001$; comparison between conditions: $^{\#}p \leqslant 0.05$, $^{\#\#}p \leqslant 0.01$, $^{\#\#\#}p \leqslant 0.001$, $^{\#\#\#\#}p \leqslant 0.0001$.

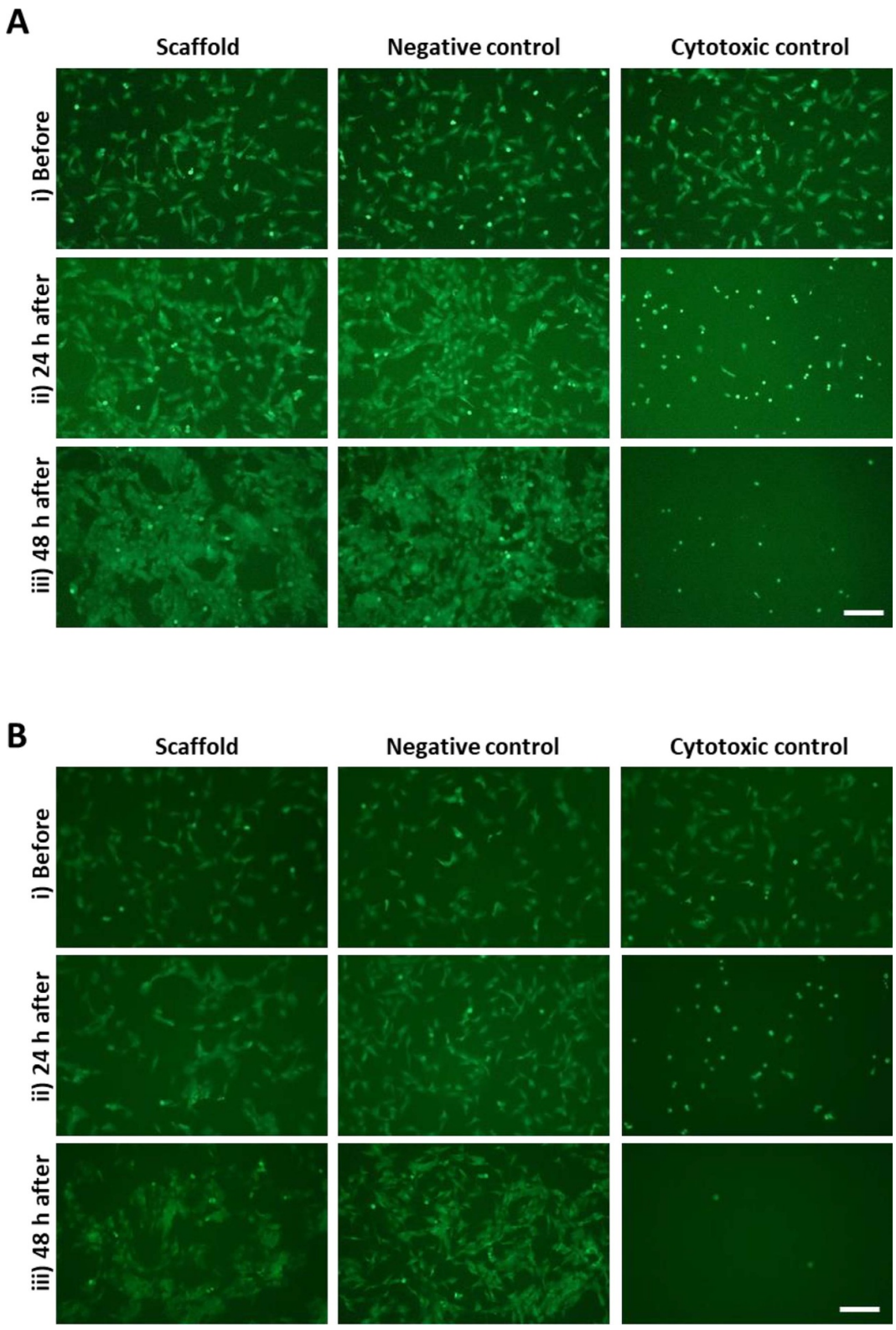

Figure 7. Microscopy analysis of MSCs treated with conditioned medium from the degradation of chitosan scaffolds. Images show cells (i) after 24 h incubation in standard medium and immediately before conditioned medium is added, (ii) 24 and (iii) 48 h after the conditioned medium was added. Conditioned medium was used from day 4 (A) and day 14 (B) after degradation and is compared with untreated medium (negative control) and with 5% DMSO medium (positive cytotoxic control). Scale bar shows 200 mm.

4. Discussion

Despite promising preclinical and clinical trials, achieving long term functional osteochondral tissue repair with tissue engineering approaches remains a challenge (GlobeNewswire 2018, Lange *et al* 2006, Christensen *et al* 2016, Verhaegen *et al* 2014). Potential tissue integration issues are being tackled

utilising multi-layered biomimetic scaffolds (Kon *et al* 2010, Kilian *et al* 2020), as recently described for a new bioresorbable chitosan construct designed as a bilayer product for osteochondral application (Pitrolino *et al* 2022). Chitosan is known to degrade into sugars, such as glucosamine, and oligosaccharides (Gorzelanny *et al* 2010), however, little is known on the precise composition and quantities released from bioresorbable chitosan scaffolds as a consequence of *in vivo* degradation (Sarem *et al* 2013, Gorczyca *et al* 2014, Nath *et al* 2015, Siddiqui *et al* 2015). It is therefore difficult to predict the local effect of molecules released from such a scaffold following its implantation. Since chitosan is known to degrade mainly by enzymatic hydrolysis, the present study investigated human chitinases such as NAG and lysozyme (Nordtveit *et al* 1996, Lim *et al* 2008). These enzymes were added to the degradation solution to mimic the *in vivo* environment, using physiological concentrations for lysozyme as found in an inflamed and damaged joint 120 mg/l (Bennett and Skoskey 1977), as well as typical levels of NAG found in the body (6.8 U/l). Mass loss, degradation products and their effect on the viability of MSCs were analysed to assess the potential of the scaffold for the treatment of osteochondral defects.

4.1. Mass loss

Chitosan polymer chains begin to break down via hydrolytic mechanisms (Roberts 1992), influenced by the DD, with DD values over 73% showing very slow degradation rates (Tomihata and Ikada 1997). The chitosan used here had a DD 84% and hence a low biodegradation rate was expected at early timepoints. Chitosan polymeric materials follow bulk erosion processes, characterised by initial swelling caused by water penetrating the core of the scaffold, before hydrolysis of the polymer network occurs (Dang *et al* 2011). Higher porosity would lead to faster degradation due to increased surface area, and the interconnected porous nature of the scaffold facilitates this rapid ingress of water and modulates bulk erosion (Dang *et al* 2011, Cunha-Reis *et al* 2007). Mechanisms for degradation involve a tri-phasic process with an initial high mass loss followed by a steady plateau, and a final accelerated mass loss stage culminating in a loss of structure and complete degradation (Ren *et al* 2005). The results presented in this study mirror the early stages of the tri-phasic model, as they also displayed a high initial mass loss followed by a plateau.

Chitosan degradation *in vivo* proceeds mainly by enzymatic hydrolysis, with little evidence for other depolymerisation processes such as acid hydrolysis or oxidative-reductive depolymerisation (Vårum *et al* 1997, Lončarević *et al* 2017). Enzymes capable of degrading chitosan include lysozyme NAG, and three human chitinases; acidic mammalian chitinase, di-N-acetylchitobiase and chitotriosidase (Kean and Thanou 2010). Both lysozyme and NAG are found in the lysosome of mammalian cells and help break down biological material. Lysozyme can be found in almost every human bodily fluid, and is present at high concentrations in the synovial fluid of inflamed joints (Bennett and Skosey 1977). NAG is secreted by kidney tubular cells and found in blood plasma (Lim *et al* 2008). Unlike ubiquitous lysozyme, the chitinases vary in prevalence throughout the human population (Boot *et al* 1998), and elevated levels seem to be specifically linked to people with Gaucher disease (Hollak *et al* 1994). Early studies in human serum found that degradation of chitosan was mediated by lysozyme rather than chitinases (Vårum *et al* 1997).

The mass loss observed here over 28 d was comparable to studies using lysozyme (Sarem *et al* 2013, Gorczyca *et al* 2014, Nath *et al* 2015) and other tissue engineered scaffolds without gelatin or collagen (Siddiqui *et al* 2015), which demonstrated a lower degradation rate than scaffolds containing gelatin or collagen. In all studies, an increase in GN concentration, used as cross-linking agent, decreased the degradation rate, most probably due to stereo hindrance, as increased GN cross-linking protects the acetyl groups from attack by lysozyme and also reduces the number of available amine groups (Gorczyca *et al* 2014, Nath *et al* 2015).

Here, lysozyme, which acts on N-acetylated and acetylated sugar units, proved a major degradation agent. Lysozyme binds to 6 sugar rings (hexameric binding) to depolymerise chitosan into mainly acetylated oligomers (Nordtveit *et al* 1996). The fastest degradation rate occurs when chitosan has 3 or 4 consecutive acetylated groups (Nordtveit *et al* 1996). Therefore, the pattern of deacetylation (PA) plays a role in degradation, and it would be interesting in the future to consider the effect of PA on the degradation kinetics and whether this could be modulated to control the degradation process. The addition of NAG showed no significant difference on the mass of either chitosan scaffold in the timeframe tested.

4.2. Scaffold mechanical properties

The ability to maintain mechanical strength post-implantation is important to the clinical suitability of a bioresorbable medical device (Cameron 2008). Here, the degradation process had no significant effect on the compressive strength or modulus of the scaffolds over the 3-week study. During the initial stages, from day 0–3 there was a slight increase in both strength and modulus, which was attributed to an increase in swelling of the scaffold after hydration (Offeddu *et al* 2018, Pitrolino *et al* 2022). This property is particularly apparent when using biomaterials (Wu *et al* 2020) and highlights the advantage of using biologically-derived materials such as chitosan. In addition, the presence of nHA in the chitosan-nHA scaffold, gave increased compressive strength (Qasim *et al* 2017).

4.3. Analysis of degradation products

Chitosan, used in pharmaceuticals and medical devices (Di Martino *et al* 2005), is biocompatible (Busilacchi *et al* 2013, Levengood and Zhang 2014), receiving GRAS (Generally Regarded as Safe) status from the FDA in 2011 (Kumar *et al* 2005). Its degradation products are mainly reducing sugars and oligosaccharides of varying molecular weight, DD and pattern of DD (Gorzelanny *et al* 2010). The present study found varying concentrations of glucose, glucosamine and N-acetyl-glucosamine released within the *in vitro* degradation timeframe tested. The sharp increase in glucosamine content at day 7 is typical of the chitosan degradation process, especially for formulations with high DD values (Ren *et al* 2005). This burst release at day 7 was preceded by a reduction in mass, possibly indicating an early release of chitosan oligosaccharides and low molecular weight chitosan. This could lead to varying concentrations of glucosamine and N-acetyl-glucosamine released in accordance with the DD value. These results provide important new data as most reports focus on a mass loss (Sarem *et al* 2013, Gorczyca *et al* 2014, Nath *et al* 2015, Siddiqui *et al* 2015) without characterising the resulting products. An increase in pH was noted at day 14, which has also been seen in other chitosan degradation studies using lysozyme, and related to the presence of cations in solution due to the dissolution of chitosan (Lončarević *et al* 2017).

4.4. Analysis of cellular response to glucosamine

When assessing the biocompatibility of chitosan scaffolds, there needs to be an assessment of the cytotoxicity of the expected degradation products. The study performed over 4 weeks showed a high concentration of glucosamine released by the degrading scaffold at day 7. The results of this study show that a similar concentration of glucosamine added to MSC culture in isolation produced a significant cytotoxic effect. Glucosamine is a widely used supplement for patients with osteoarthritis, and several studies performed *in vitro* on chondrocytes and stem cells reported a dose-dependent effect of glucosamine leading to either a chondroprotective or a cytotoxic effect (de Mattei *et al* 2002, Dodge and Jimenez 2003, Derfoul *et al* 2007, Shikhman *et al* 2009). For example, *in vitro* studies on chondrocytes found increased levels of the proteoglycan aggrecan and decreased levels of the matrix degrading enzymes MMP-3 and MMP-13, when exposed to glucosamine at doses between 1–150 μM (Dodge and Jimenez 2003, Derfoul *et al* 2007). However, higher glucosamine doses between 1–100 mM exerted a cytotoxic effect on chondrocytes and stem cells (de Mattei *et al* 2002, Derfoul *et al* 2007, Shikhman *et al* 2009). These studies point to the participation of glucosamine in the hexosamine biosynthetic pathway, responsible for the production of glycosaminoglycans and cytoskeleton proteins through the metabolism of glucose. They suggest lower glucosamine concentrations could increase levels of UDP-NAGluc and stimulate GAG synthesis (Dodge and Jimenez 2003), while higher concentrations may block glucose transport and lead to cell death (Shikhman *et al* 2009). The high concentrations of glucosamine released from the chitosan scaffolds in this study ($>$ 100 mM), and the subsequent cytotoxic effect on cells observed *in vitro*, are aligned with previous *in vitro* trials with high concentrations of glucosamine (1–100 mM) (de Mattei *et al* 2002, Derfoul *et al* 2007, Shikhman *et al* 2009). For future iterations of chitosan scaffold design, it will be important to consider the glucosamine release kinetics to modulate possible effects of this degradation product on the surrounding tissue.

4.5. Analysis of cellular response to degradation supernatant—cytotoxicity

The cytotoxicity of chitosan scaffolds was measured by exposing MSCs to scaffold degradation extracts to estimate the local effects of the implant degradation *in vivo*. A decrease in metabolic activity was noticed in response to day 14 extracts, which coincided with a transient decrease in cell number, suggesting a negative effect on the cells from the degradation supernatant at this time-point, which could result from the released products including glucosamine, glucose and N-acetyl-glucosamine identified in this study. The added effect of other degradation products and chitosan oligosaccharides not identified here cannot be discounted, as well as the effect of the resulting drop in pH. N-acetyl-glucosamine was present at concentrations close to 3 mM at days 7, 14 and 21, which previous studies linked to a chondroprotective effect, showing increased GAG synthesis, increased glucose transport and higher levels of ATP (Shikhman *et al* 2009). Since the cell cultures appeared to increase in cell number after the initial incubation period, it is likely that any potential cytotoxic effect, possibly due to glucosamine burst release, could be dissipated, leading to recovery of cell growth. The influence of released chitosan oligosaccharides is uncertain, and additional work characterising degradation products from chitosan scaffolds is needed to better assess the effect of degradation products on the surrounding tissue, and on the osteogenic differentiation of mesenchymal progenitors, to better evaluate the performance of these scaffolds for osteochondral use.

An in-silico approach, predicting the combinations of oligosaccharides released, may be useful to model the degradation kinetics from chitosan devices, especially those with differing degrees and patterns of deacetylation (Gorzelanny *et al* 2010). In addition, the kinetics of nHA release over time, and its possible

pro-osteogenic effects, would provide complementary information on the likely effect of a degrading chitosan-nHA scaffold on local cell progenitors.

5. Conclusion

The degradation profile of a new bilayer chitosan scaffold developed for osteochondral applications has been analysed *in vitro*, using a novel combination of lysozyme and NAG enzymes. The chitosan scaffold was observed to slowly degrade by bulk erosion processes and hydrolytic mechanisms. Exposure to the selected enzymes, which are present in a human joint, resulted in an increased degradation rate compared to PBS controls, producing a model relevant to the *in vivo* environment. The main degradation products identified and quantified showed a burst release at early timepoints, with concentrations of glucosamine peaking at day 7 to reach 2–200 mM. These concentrations were observed to have a negative effect on MSC cultures. The results illustrate the need to better control the degradation profile of chitosan scaffolds to mitigate the potential accumulation of glucosamine surrounding bioresorbable implants.

Data availability statement

The data cannot be made publicly available upon publication because no suitable repository exists for hosting data in this field of study. The data that support the findings of this study are available upon reasonable request from the authors.

Acknowledgments

This work was supported by the UK Engineering and Physical Sciences Research Council (EPSRC) Centre for Doctoral Training [Grant Numbers EP/F500491/1], the EPSRC Centre for Innovative Manufacturing for Medical Devices [Grant Numbers EP/K029592/1]. This report describes work conducted under the Medical Technologies Innovation and Knowledge Centre's Proof of Concept programme, funded by the EPSRC [Grant Number POC062]. This work was supported by Versus Arthritis [Grant Number 21501]. VS is funded by a grant from the Italian Ministry of University and Research (MUR) to the Department of Molecular Medicine (University of Pavia) under the 'Dipartimenti di Eccellenza (2023–2027)' initiative.

Author contributions

All authors contributed to the study conception and design. Material preparation and data collection were performed by K P and R F. Data analysis and interpretation was performed by K P, R F, C S, D G and V S. The manuscript was written by K P and V S with input from other authors.

Conflict of interest

The authors have no relevant financial or non-financial interests to disclose.

ORCID iDs

David Grant https://orcid.org/0000-0002-6786-7720
Virginie Sottile https://orcid.org/0000-0002-6064-5738

References

Angolkar M, Paramshetti S, Gahtani R M, Al Shahrani M, Hani U, Talath S, Osmani R A M, Spandana A, Gangadharappa H V and Gundawar R 2024 Pioneering a paradigm shift in tissue engineering and regeneration with polysaccharides and proteins-based scaffolds: a comprehensive review *Int. J. Biol. Macromol.* **265** 130643

Bedi A, Feeley B T and Williams R J 3rd 2010 Management of articular cartilage defects of the knee *J. Bone Joint Surg. Am.* **92** 994–1009

Bennett R M and Skosey J L 1977 Lactoferrin and lysozyme levels in synovial fluid *Arthritis Rheum.* **20** 84–90

Boot R G, Renkema G H, Verhoek M, Strijland A, Bliek J, de Meulemeester T M, Mannens M M and Aerts J M 1998 The human chitotriosidase gene. Nature of inherited enzyme deficiency *J. Biol. Chem.* **273** 25680–5

Busilacchi A, Gigante A, Mattioli-Belmonte M, Manzotti S and Muzzarelli R A A 2013 Chitosan stabilizes platelet growth factors and modulates stem cell differentiation toward tissue regeneration *Carbohydr. Polym.* **98** 665–76

Cameron R E 2008 *Degradation Rate of Bioresorbable Materials: Prediction and Evaluation/edited by Fraser Buchanan* Ed. F Buchanan (CRC Press) pp 43–66

Christensen B B, Foldager C B, Jensen J, Jensen N C and Lind M 2016 Poor osteochondral repair by a biomimetic collagen scaffold: 1- to 3-year clinical and radiological follow-up *Knee Surg. Sports Traumatol. Arthrosc.* **24** 2380–7

Collins M N, Ren G, Young K, Pina S, Reis R L and Oliveira J M 2021 Scaffold fabrication technologies and structure/function properties in bone tissue engineering *Adv. Funct. Mater.* **31** 2010609

Croisier F and Jérôme C 2013 Chitosan-based biomaterials for tissue engineering *Eur. Polym. J.* **49** 780–92

Cunha-Reis C, TuzlaKoglu K, Baas E, Yang Y, Haj A E and Reis R L 2007 Influence of porosity and fibre diameter on the degradation of chitosan fibre-mesh scaffolds and cell adhesion *J. Mater. Sci.: Mater. Med.* **18** 195–200

Dang Q F, Yan J Q, Li J J, Cheng X J, Liu C S and Chen X G 2011 Controlled gelation temperature, pore diameter and degradation of a highly porous chitosan-based hydrogel *Carbohydr. Polym.* **83** 171–8

de Mattei M, Pellati A, Pasello M, de Terlizzi F, Massari L, Gemmati D and Caruso A 2002 High doses of glucosamine-HCl have detrimental effects on bovine articular cartilage explants cultured in vitro *Osteoarthr. Cartil.* **10** 816–25

Derfoul A, Miyoshi A D, Freeman D E and Tuan R S 2007 Glucosamine promotes chondrogenic phenotype in both chondrocytes and mesenchymal stem cells and inhibits MMP-13 expression and matrix degradation *Osteoarthritis Cartilage* **15** 646–55

Di Martino A, Sittinger M and Risbud M V 2005 Chitosan: a versatile biopolymer for orthopaedic tissue-engineering *Biomaterials* **26** 5983–90

Dodge G R and Jimenez S A 2003 Glucosamine sulfate modulates the levels of aggrecan and matrix metalloproteinase-3

synthesized by cultured human osteoarthritis articular chondrocytes *Osteoarthr. Cartil.* **11** 424–32
Felfel R M, Gupta D, Zabidi A Z, Prosser A, Scotchford C A, Sottile V and Grant D M 2018 Performance of multiphase scaffolds for bone repair based on two-photon polymerized poly(d,l-lactide-co-ε-caprolactone), recombinamers hydrogel and nano-HA *Mater. Des.* **160** 455–67
Fourie J, Taute F, du Preez L and De Beer D 2022 Chitosan composite biomaterials for bone tissue engineering—a review *Regen. Eng. Transl. Med.* **8** 1–21
GlobeNewswire 2018 Histogenics announces top-line results from phase 3 clinical trial *GlobeNewswire* (available at: www.globenewswire.com/news-release/2018/09/05/1565410/0/en/Histogenics-Announces-Top-Line-Results-From-Phase-3-Clinical-Trial-of-NeoCart-in-Patients-With-Knee-Cartilage-Damage.html) (Accessed 24 February)
Gorczyca G, Tylingo R, Szweda P, Augustin E, Sadowska M and Milewski S 2014 Preparation and characterization of genipin cross-linked porous chitosan-collagen-gelatin scaffolds using chitosan-CO2 solution *Carbohydr. Polym.* **102** 901–11
Gorzelanny C, Pöppelmann B, Pappelbaum K, Moerschbacher B M and Schneider S W 2010 Human macrophage activation triggered by chitotriosidase-mediated chitin and chitosan degradation *Biomaterials* **31** 8556–63
Harrison R, Markides H, Morris R H, Richards P, El Haj A J and Sottile V 2017 Autonomous magnetic labelling of functional mesenchymal stem cells for improved traceability and spatial control in cell therapy applications *J. Tissue Eng. Regen. Med.* **11** 2333–48
Hollak C E, van Weely S, van Oers M H and Aerts J M 1994 Marked elevation of plasma chitotriosidase activity. A novel hallmark of Gaucher disease *J. Clin. Invest.* **93** 1288–92
Hulsart-Billström G *et al* 2016 A surprisingly poor correlation between in vitro and in vivo testing of biomaterials for bone regeneration: results of a multicentre analysis *Eur. Cells. Mater.* **31** 312–22
Kean T and Thanou M 2010 Biodegradation, biodistribution and toxicity of chitosan *Adv. Drug Deliv. Rev.* **62** 3–11
Kilian D, Ahlfeld T, Akkineni A R, Bernhardt A, Gelinsky M and Lode A 2020 3D Bioprinting of osteochondral tissue substitutes–in vitro-chondrogenesis in multi-layered mineralized constructs *Sci. Rep.* **10** 8277
Kon E, Delcogliano M, Filardo G, Pressato D, Busacca M, Grigolo B, Desando G and Marcacci M 2010 A novel nano-composite multi-layered biomaterial for treatment of osteochondral lesions: technique note and an early stability pilot clinical trial *Injury* **41** 693–701
Koons G L, Diba M and Mikos A G 2020 Materials design for bone-tissue engineering *Nat. Rev. Mater.* **5** 584–603
Kumar M N V R, Muzzarelli R A A, Muzzarelli C, Sashiwa H and Domb A J 2005 Chitosan Chemistry and Pharmaceutical Perspectives *ChemInform* **36** 11
Lange J, Follak N, Nowotny T and Merk H 2006 Results of SaluCartilage implantation for stage IV chondral defects in the knee joint area *Der Unfallchirurg* **109** 193–9
Levengood S L and Zhang M 2014 Chitosan-based scaffolds for bone tissue engineering *J. Mater. Chem. B Mater. Biol. Med.* **2** 3161–84
Lim S M, Song D K, Oh S H, Lee-Yoon D S, Bae E H and Lee J H 2008 In vitro and in vivo degradation behavior of acetylated chitosan porous beads *J. Biomater. Sci. Polym. Ed.* **19** 453–66
Lončarević A, Ivanković M and Rogina A 2017 Lysozyme-induced degradation of chitosan: the characterisation of degraded chitosan scaffolds *J. Tissue Repai Regeneration* **1** 12–22
Macri-Pellizzeri L, Melo N D, Ahmed I, Grant D, Scammell B and Sottile V 2018 Live quantitative monitoring of mineral deposition in stem cells using tetracycline hydrochloride *Tissue Eng. Part C Methods* **24** 171–8
Marshall K M *et al* 2023 Bioactive coatings on 3D printed scaffolds for bone regeneration: use of Laponite™ to deliver BMP-2 for bone tissue engineering—progression through in vitro, chorioallantoic membrane assay and murine subcutaneous model validation *bioRxiv Preprint* https://doi.org/10.1101/2023.10.25.560313
Martinez A, Blanco M D, Davidenko N and Cameron R E 2015 Tailoring chitosan/collagen scaffolds for tissue engineering: effect of composition and different crosslinking agents on scaffold properties *Carbohydr. Polym.* **132** 606–19
McCarrel T M, Pownder S L, Gilbert S, Koff M F, Castiglione E, Saska R A, Bradica G and Fortier L A 2017 Two-year evaluation of osteochondral repair with a novel biphasic graft saturated in bone marrow in an equine model *Cartilage* **8** 406–16
McCarthy H S and Roberts S 2013 A histological comparison of the repair tissue formed when using either Chondrogide® or periosteum during autologous chondrocyte implantation *Osteoarthritis Cartilage* **21** 2048–57
Nath S D, Abueva C, Kim B and Lee B T 2015 Chitosan-hyaluronic acid polyelectrolyte complex scaffold crosslinked with genipin for immobilization and controlled release of BMP-2 *Carbohydr. Polym.* **115** 160–9
Nawaz S Z, Bentley G, Briggs T W R, Carrington R W J, Skinner J A, Gallagher K R and Dhinsa B S 2014 Autologous chondrocyte implantation in the knee: mid-term to long-term results *JBJS* **96** 824–30
Nordtveit R J, Varum K M and Smidsrod O 1996 Degradation of partially N-acetylated chitosans with hen egg white and human lysozyme *Carbohydr. Polym.* **29** 163–7
Notara M, Scotchford C A, Grant D M, Weston N and Roberts G A 2009 Cytocompatibility and hemocompatibility of a novel chitosan-alginate gel system *J. Biomed. Mater. Res.* **89** 854–64
Offeddu G S, Tanase C E, Toumpaniari S, Oyen M L and Cameron R E 2018 Stiffening by osmotic swelling constraint in cartilage-like cell culture scaffolds *Macromol. Biosci.* **18** 1800247
Piaia L, Silva S S, Fernandes E M, Gomes J M, Franco A R, Leonor I B, Fredel M C, Salmoria G V, Hotza D and Reis R L 2024 Chitosan-based hierarchical scaffolds crosslinked with genipin *J. Compos. Sci.* **8** 85
Pitrolino K A, Felfel R M, Pellizzeri L M, Mlaren J, Popov A A, Sottile V, Scotchford C A, Scammell B E, Roberts G A F and Grant D M 2022 Development and in vitro assessment of a bi-layered chitosan-nano-hydroxyapatite osteochondral scaffold *Carbohydr. Polym.* **119126** 119126
Qasim S B, Husain S, Huang Y, Pogorielov M, Deineka V, Lyndin M, Rawlinson A and Rehman I U 2017 In-vitro and in-vivo degradation studies of freeze gelated porous chitosan composite scaffolds for tissue engineering applications *Polym. Degrad. Stab.* **136** 31–38
Ren D, Yi H, Wang W and Ma X 2005 The enzymatic degradation and swelling properties of chitosan matrices with different degrees of N-acetylation *Carbohydr. Res.* **340** 2403–10
Roberts G A F 1992 *Chitin Chemistry* vol 1 (Macmillian)
Sarem M, Moztarzadeh F and Mozafari M 2013 How can genipin assist gelatin/carbohydrate chitosan scaffolds to act as replacements of load-bearing soft tissues? *Carbohydr. Polym.* **93** 635–43
Schneider U, Rackwitz L, Andereya S, Siebenlist S, Fensky F, Reichert J, Loer I, Barthel T, Rudert M and Noth U 2011 A prospective multicenter study on the outcome of type I collagen hydrogel-based autologous chondrocyte implantation (CaReS) for the repair of articular cartilage defects in the knee *Am. J. Sports Med.* **39** 2558–65
Shikhman A R, Brinson D C, Valbracht J and Lotz M K 2009 Differential metabolic effects of glucosamine and N-acetylglucosamine in human articular chondrocytes *Osteoarthritis Cartilage* **17** 1022–8
Siddiqui N, Pramanik K and Jabbari E 2015 Osteogenic differentiation of human mesenchymal stem cells in freeze-gelled chitosan/nano beta-tricalcium phosphate porous scaffolds crosslinked with genipin *Mater. Sci. Eng. C. Mater. Biol. Appl.* **54** 76–83
Stanish W D, McCormack R, Forriol F, Mohtadi N, Pelet S, Desnoyers J, Restrepo A and Shive M S 2013 Novel

scaffold-based BST-CarGel treatment results in superior cartilage repair compared with microfracture in a randomized controlled trial *J. Bone Joint Surg. Am.* **95** 1640–50

Thein-Han W W and Misra R D 2009 Biomimetic chitosan-nanohydroxyapatite composite scaffolds for bone tissue engineering *Acta Biomater.* **5** 1182–97

Tomihata K and Ikada Y 1997 In vitro and in vivo degradation of films of chitin and its deacetylated derivatives *Biomaterials* **18** 567–75

Tribe H C, McEwan J, Taylor H, Oreffo R O C and Tare R S 2017 Mesenchymal stem cells: potential role in the treatment of osteochondral lesions of the ankle *Biotechnol. J.* **12** 1700070

Vårum K M, Myhr M M, Hjerde R J N and Smidsrød O 1997 In vitro degradation rates of partially N-acetylated chitosans in human serum *Carbohydr. Res.* **299** 99–101

Verhaegen J, Clockaerts S, Van Osch G J V M, Somville J, Verdonk P and Mertens P 2014 TruFit plug for repair of osteochondral defects—where is the evidence? systematic review of literature *Cartilage* **6** 12–19

Wu F, Pang Y and Liu J 2020 Swelling-strengthening hydrogels by embedding with deformable nanobarriers *Nat. Commun.* **11** 4502

Wylie J D, Hartley M K, Kapron A L, Aoki S K and Maak T G 2016 Failures and reoperations after matrix-assisted cartilage repair of the knee: a systematic review. *arthroscopy J. Arthrosc. Relat. Surg.* **32** 386–92